SIZE AND EFFICIENCY BASED COMPARISON OF KINEMATICALLY EQUIVALENT TWO-CARRIER PLANETARY GEAR TRAINS

Željko Vrcan[1*] – Vladislav Ivanov[2] – Angel Alexandrov[2] – Madina Isametova[3]

[1]Department of Mechanical Engineering Design, Faculty of Engineering, University of Rijeka, Vukovarska 58, HR-51000 Rijeka, Croatia
[2]Department of Machine Elements and Non-metallic constructions, Faculty of Mechanical Engineering, Technical University of Sofia, 8 Kliment. Ohridski Boulevard, BG-1756 Sofia, Bulgaria
[3]Department of Mechanical Engineering, Standardization, Certification and Metrology, Institute of Energy and Mechanical Engineering, Satbayev University, Satpaev Street 22a, KZ-050013, Almaty, Kazakhstan

ARTICLE INFO

***Article history*:**
Received: 05.07.2022
Received in revised form: 22.07.2022
Accepted: 19.09.2022.

Keywords:
Two-carrier planetary gear train
Efficiency
Transmission ratio
Power to Weight Ratio
Kinematic Analysis

DOI: https://doi.org/10.30765/er.1989

Abstract:

The subject of this paper is a two-carrier planetary gear train (PGT) which was developed for a specific purpose. This PGT may be used for applications in which a negative transmission ratio in the range -3…-143 is required. In this case, the mechanical and dimensional properties of the PGT have been analysed for nominal negative transmission ratios of -30 and -40. All possible combinations of simple component PGT ideal torque ratios providing those transmission ratios were obtained. Only the combinations providing the minimum radial dimensions of the PGT assembly were selected. Subsequent analysis has shown that the PGT radial dimensions will be minimised when the ratio of the reference diameters of the planetary unit ring gears is close to unity, meaning that the PGT casing will be cylindrical rather than stepped. This paper also provides an overview of the DVOBRZ software package used to synthesize the different gearbox layouts for the required transmission ratio, combined with a basic introduction to single speed two-carrier PGTs for better understanding. The DVOBRZ software was used to select all the acceptable gearboxes were selected from the set of generated PGTs according to the criteria of minimum dimensions and acceptable efficiency range. This set of PGTs was checked for kinematic feasibility and construction concepts were created for feasible layouts.

1 Introduction

Mechanical power transmissions must be present in some form in all machines, as mechanical energy must be transferred from the prime mover to the working end of the machine. The transmission is also used to provide other useful functions, notably to adjust the magnitude of the force or torque provided by the prime mover to the demands of the driven machine [1], [2].

Some of the most used forms of power transmission use gears, with planetary gear trains (PGTs) being a special type with several advantages in comparison to conventional geared units. The most known advantage is a compactness of design and improvements in durability and reliability due to the benefits of power being split over several planet gears. This may be even further enhanced by applications of vibration analysis and development of customized bearing solutions [3] - [11] resulting in the design of PGTs with high power ratings applicable in a wide range of transmission ratios. However, complex kinematic schemes which require manual

* Corresponding author
E-mail address: zeljko.vrcan@riteh.hr

validation and the need for intricate calculations in comparison to conventional gearboxes, mean that systematic research is required to unlock the full engineering potential of planetary gearboxes [12], [13].

Current industrial applications use transmission ratios in the range i =18…90 [9]. The basic type of PGT designated 1AI according to the German classification system is commonly applied in the range i = 3…8 (exceptionally up to i = 12). Therefore, the required transmission ratio range can be achieved only by combining two PGTs of the basic into a compound PGT [10]-[14].

The relatively small size and high reliability of gearboxes using such compound PGTs has resulted in a range of applications in hoisting and transportation technology. Another important area of application is found in machine tool gearboxes, where two-carrier two-speed PGTs with brakes on coupled shafts may be used [15]. This type of compound PGT may be even optimized for marine propulsion [16].

Planetary gear trains have also been widely used in the aviation industry ever since the 1930s, mostly due to their small encumbrance, quiet and smooth operation, high loading capacity and long service life. This has also required methods for predicting the reliability of planetary gear trains in partial load state, as presented in [17].

The automobile and automation industries also present an important are for the application of PGTs. Notably, automatic transmissions may contain any number of simple, compound or complex-compound planetary gear sets [18], while new concepts for the calculation of internal power flows, i.e., the split-power ratio and the virtual split-power ratio, have been introduced and presented in [19]. The high power-to-weight ratio and small encumbrance of PGTs in addition to the possibility to design and operate a multi speed transmission, make them highly suitable for electric vehicles, with a hybrid dynamic model for PGTs using helical gears and operating in conditions of high and variable input speed proposed in [20].

Until now, two-carrier PGTs have not been widely researched, and most has been done in a sporadic manner. However, multi-carrier PGTs have been the subject of some systematic research in the last ten years or so. Structural connections between the component gear trains have been systematically researched, with methodology being provided to apply lever analogy to the determination of transmission ratios and efficiency calculations [21]. The kinematic properties of multi-carrier PGTs have been extensively researched in [22], [23], while the torque method was used to determine efficiencies of single and two-speed PGTs [24], [25].

The research carried out in [9] was also used to develop the DVOBRZ software used in the research presented in this paper. The application of this software has enabled two-carrier PGTs to be optimally synthesised, analysed, and selected.

The mechanical and dimensional characteristics of PGTs for nominal negative transmission ratios of -30 and -40 have been considered, with several combinations of ideal torque ratios of the component PGT being obtained. The combinations providing the minimum radial dimensions of the planetary gear units were then selected, before being filtered according to the criteria of acceptable efficiency. The accepted solutions were kinematically checked and their internal layout concepts created.

2 Research of two-carrier, single speed planetary gear trains

The research presented in this paper deals with a particular configuration of single speed two-carrier PGTs. The constraints of the application demand kinematically negative transmission ratios of -30 and -40, with the added requirement that the component PGTs be similar in size for the casing to have the simplest possible shape. This will in turn minimize manufacturing costs.

The casing can achieve a cylindrical shape if the ratio of the ring gear diameters is close to one, and the relation to ring gear diameters must be considered because of this.

The simplest PGT, 1AI is used for both component gear trains (Figure 1). The construction is relatively simple with only three parts, the sun gear 1, the planet gears 2, the annulus (ring gear) 3 and planet carrier S. The specific torques on its shafts and its matching Wolf-Arnaudov symbol are also shown in Figure 1. [13].

The Wolf-Arnaudov symbol presents a simplified form of the PGT with train shafts represented by lines of different thickness protruding from a circle. The sun gear shaft 1 is represented by a thin line, the planet carrier shaft S by two parallel lines, and the ring gear shaft 3 by a thick line. The summary element is the element which creates a negative transmission ratio when locked and is marked with two parallel lines. In the case of 1AI, the carrier shaft is the summary element because a negative transmission ratio is obtained by locking the planet carrier.

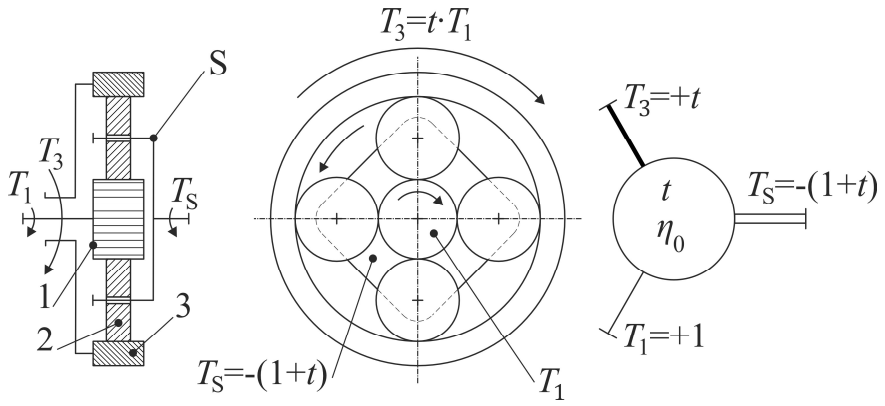

Figure 1. Schematic of 1AI (left), Specific torques on the shafts of 1AI (center) and Wolf-Arnaudov symbol of 1AI (right).

The ideal torque ratio t of the PGT is given by Eq. (1), and the shaft torque ratio is given by Eq. (2), where z_1 is the number of teeth of the sun gear, z_3 is the number of teeth of the ring gear, T_1 is the torque acting on the sun gear shaft 1, T_3 is the torque acting on the ring gear shaft 3, T_S is the torque acting on the planet carrier shaft S, and T_D is the differential torque:

$$t = \frac{T_3}{T_1} = \frac{T_{D\max}}{T_{D\min}} = \frac{|z_3|}{z_1} > +1 \tag{1}$$

$$T_1 : T_3 : T_S = +1 : +t : -(1+t) \tag{2}$$

Multi-carrier PGTs are created by connecting the shafts of simple PGTs such as 1AI [11]. As this paper deals with two-carrier PGTs, two-carrier PGTs with three external shafts composed of two basic PGTs and having a fixed transmission ratio will be considered. In this case, two of the three external shafts are single shafts, while the third one is a compound shaft, as indicated in Figure 2.

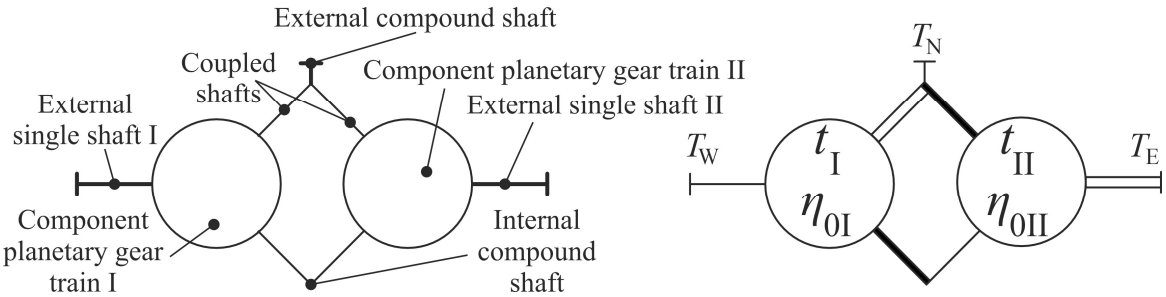

Figure 2. Symbolic view of two-carrier PGT with shafts and respective torques marked.

The cardinal directions are used to mark the external shafts (W, N, E), and the external shaft torques have been designated accordingly (T_W, T_N and T_E). The shafts are always sequenced power input to power output. The symbol is also marked with the ideal torque ratio (t_I and t_{II}) and efficiency (η_{0I} and η_{0II}) for every basic component PGT [16].

It is possible to connect every component PGT in six different ways, depending on which shaft is assigned to each cardinal direction. For example, by placing the sun gear shaft of component gear train 1 to west, two combinations are created with the planet carrier and ring gear shafts at north and south. The other four combinations are then achieved by alternately placing the planet carrier and ring gear shafts to west.

The same is achieved for component gear train 2 by placing two shafts to north and south respectively, with the combination determined by the east shaft. By repeating this procedure for all six positions of the

component gear trains, a total of 36 different PGT layouts can be achieved in this manner, however in practice this is reduced to a total of 21 due to the isomorphous characteristics of some layouts. An overview of their structures and the logic of their assembly can be observed in Figure 3 [13]. Furthermore, every compound PGT shown in Figure 3 can be operated in six different modes, as any external shaft can be made stationary, with the other two external shafts acting as either input or output, resulting in a total of 126 different transmission variants [13].

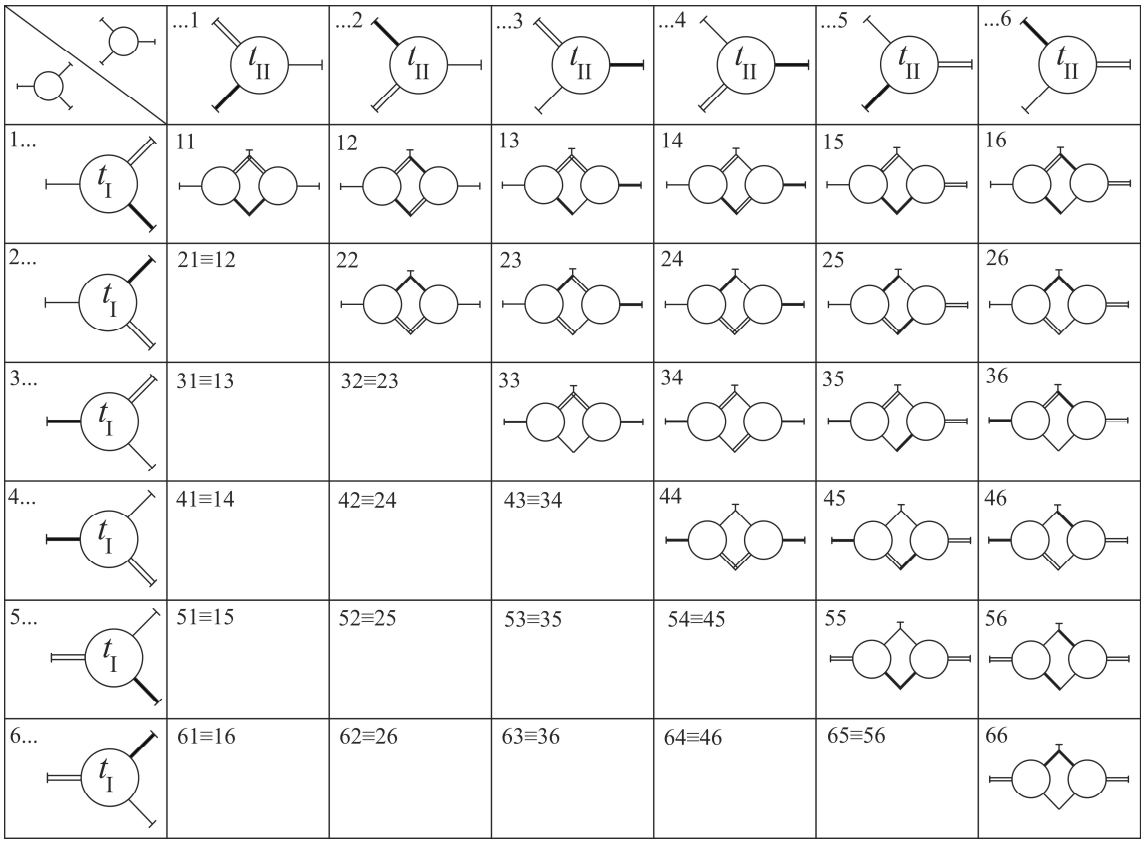

Figure 3. Overview of PGT layouts.

A matrix type designation is used to annotate the scheme and its operating mode (for example, S45 – line 4, column 5). The power input and output are designated using cardinal directions, and the stationary element is placed in parentheses. Therefore, S45NE(W) means layout 45 with the power flow from the northern input shaft to the eastern output shaft with the western shaft locked. As it has been already stated that the PGT has three external shafts and the internal shaft is always placed south by convention, it is enough to write just S45NE to fully designate a PGT.

3 Application of the DVOBRZ computer program

The principle of operation of the DVOBRZ software was explained in detail in [26], however as it was used to identify valid solutions under application constraints, a flowchart of the program is given in Figure 4 together with a brief explanation of the principle of operation of the software will be given.

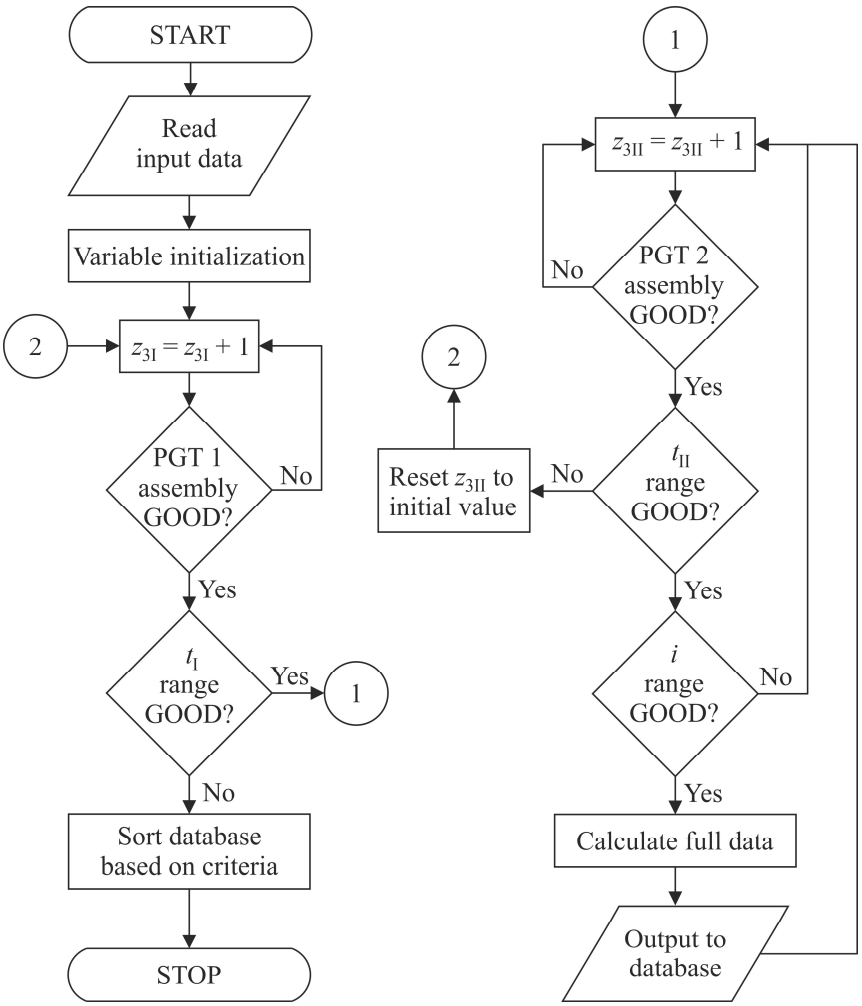

Figure 4. Flow chart of the DVOBRZ software.

The program was developed to identify the variants of two-carrier PGTs and their parameters that fulfil the kinematic requirements before listing them in order of priority according to the selection criteria [27], [28], such as maximum efficiency, minimum weight, or size constraints. The program is capable of tabulating solutions for two-speed and single-speed gearboxes, depending on whether the actual gearbox will have a fixed transmission ratio, or a transmission ratio change mechanism [29].

During operation, the program checks the ideal torque ratios of every possible combination of simple component gear trains, discarding those outside the required transmission ratio range. The transmission ratio of both gear trains is calculated for every possible combination of ideal torque ratios and then checked whether the result is within the tolerance range for the desired transmission ratios.

The ideal torque ratios are represented by means of the numbers of teeth on sun and ring gears for both component gear trains (Eq. 3 and Eq. 4):

$$t_{\mathrm{I}} = \frac{|z_{3\mathrm{I}}|}{z_{1\mathrm{I}}} \tag{3}$$

$$t_{\mathrm{II}} = \frac{|z_{3\mathrm{II}}|}{z_{1\mathrm{II}}} \tag{4}$$

The tooth numbers of the sun gears z_{1I} and z_{1II} are user set before initializing the program. One ring gear (usually z_{3I}) is then enlarged by one tooth and checked whether the ideal torque ratio is valid, which is true if the simple component gear train satisfies the assembly conditions. If it does not, the data is discarded, and another tooth is added to the ring gear. This procedure is repeated until the program finds a valid ideal torque ratio or reaches the highest possible ideal torque ratio for that component gear train. The exact procedure is then applied to the second component gear train.

The values of different parameters for each valid member of the set of ratios (basic geometry of component gear trains, component efficiency, transmission ratios, overall efficiency for each transmission ratio etc.) are calculated and stored as a function of the ideal torque ratios of the component gear trains t_I and t_{II}. The resulting database is then searched for the best gearbox variant, either by a single criterion [30], [31] (overall efficiency, minimal ratio of ring gear reference diameters, reference diameter of the largest ring gear etc.), or by multi-criteria optimization. In the latter case, the weighting coefficients for each optimization criteria are determined according to the importance of each criterion is for the application demand.

However, any selected layout variant must pass a manual check of its kinematic scheme to check out whether the solution is valid, and within the relevant design and manufacturing criteria [32]. This kinematic check consists of a schematic of the PGT being drawn up to verify whether the component PGTs may be interconnected in the intended manner, as some layouts can be impossible to assemble due to difficult bearing placement and intersections of internal and/or locked shafts. Furthermore, some layouts require a complex multiple hollow shaft design which may be very hard to manufacture.

The design parameters applied to the PGTs covered in this paper were determined from constraints suggested in the literature. It was assumed that all gears will be made from the same material.

A summary of the most important input data is provided: number of teeth of the first sun gear $z_{1I} = 21$ (user selected value), number of teeth of the second sun gear $z_{1II} = 21$ (user selected value), number of planets in each PGT $k = 3$ (application demand), gears manufactured using 16MnCr4 steel (application demand), average value of planet bearing losses coefficient $k_b = 0.065$ [9], [11], average value of seal frictional losses coefficient $k_s = 0.05$ [9], [11], average value of churning losses coefficient $k_c = 0.125$ [9], [11], gear width to diameter ratio $b / d_1 = 0.7$ (user selected value), overall efficiency $\eta \geq 0.93$ (application demand).

3.1 Application example 1

The analysis in example 1 was performed for the overall transmission ratio $i = -30$. 16 transmission layouts fulfilling the demands were discovered, however isomorphy has reduced this down to 10 different variants. The schematics of these variants are given in Figure 5.

The analysis of the program results has shown that optimization for maximum efficiency provides a negligible increase in efficiency in relation to the solution for minimal dimensions, however the outside diameters of the component PGTs will be different, pointing to the conclusion that it is best to optimise for equal outside diameters. The outside diameters will be approximately equal when the relation of maximal and minimal values of outside diameters of the two component gear trains becomes close to unity.

The research results are presented in Table 1 according to the following criteria: housing shape, maximum transmission diameter and transmission efficiency.

The variant S13WN shown in Figure 6 was selected as the optimal solution. Its internal power circulation is insignificant [33], the gear train is easy to build, and it has already been extensively covered in available literature [34].

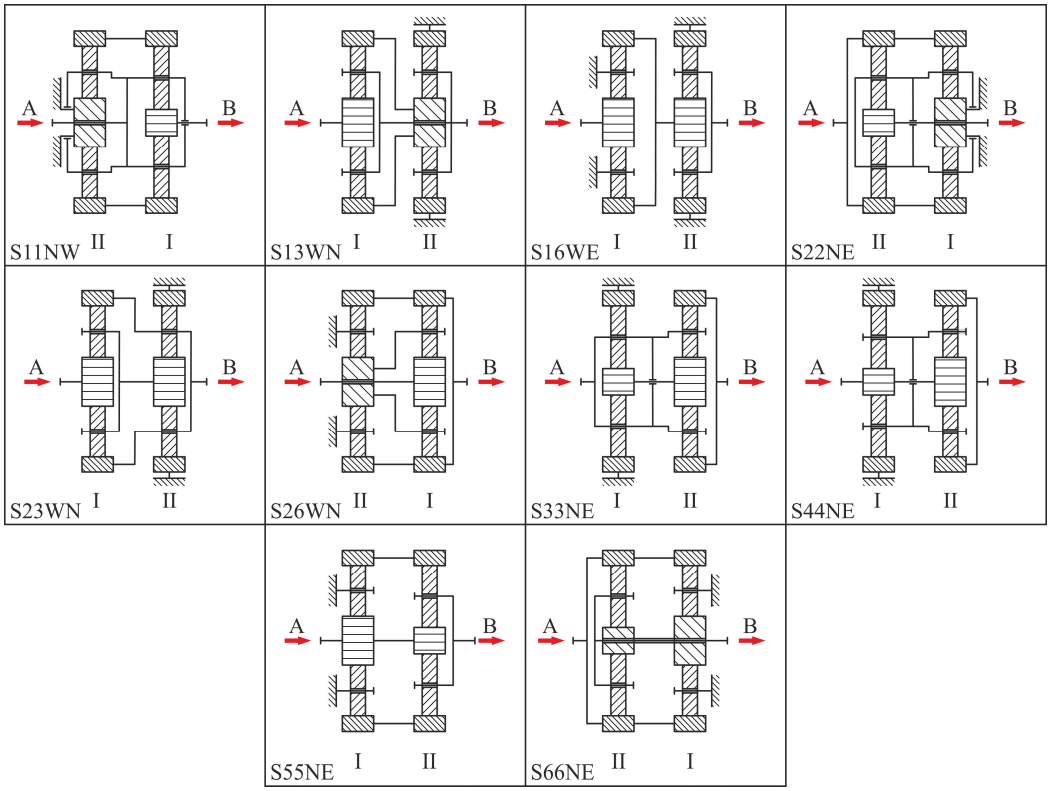

Figure 5. Applicable variants of single speed transmissions.

Table 1. Tabulated research results for i = -30.

Variant	t_I	t_{II}	d_{max}/d_{min}	d_{max}	η	m_I	m_{II}
S66NE	4	3.83	1.043	216	0.52	3	3
S55NE	3.17	3.67	1.081	231	0.77	3.75	3.5
S26WN	6.5	3	1.020	234	0.97	2	4.25
S16WE	6.83	3.33	1.025	246	0.97	2	4
S44NE	3.67	3.17	1.022	247.5	0.77	3.75	4.25
S23WE	7.33	3.5	1.014	267.7	0.97	2	4.25
S33NE	5.17	5	1.033	279	0.50	3	3
S13WN	7.83	3.83	1.022	282	0.97	2	4
S22NE	4	4.17	1.008	378	0.52	5.25	5
S11NW	5	4.83	1.017	435	0.50	4.75	5

Gear train S13WN is composed of component gear trains I and II. Power input is through sun gear I (1), with planet carriers I (2) and II (3) connected to a common shaft (4) for power output. Planet carriers I and II are connected by this shaft passing through hollow sun gear II (5) connected to ring gear I (6). Ring gear I is supported by a large rolling bearing (7), and ring gear II (8) is permanently locked to the gear train casing (9).

The internal power flow direction is displayed in Fig. 7. Power enters by means of the sun gear I and exits component PGT I by means of the ring gear I connected to sun gear II. The locked ring gear II provides reactive torque to PGT II, and power exits by means of the common carrier shaft connecting carriers I and II. The carrier shaft itself carries the required amount of circulating power back to carrier I.

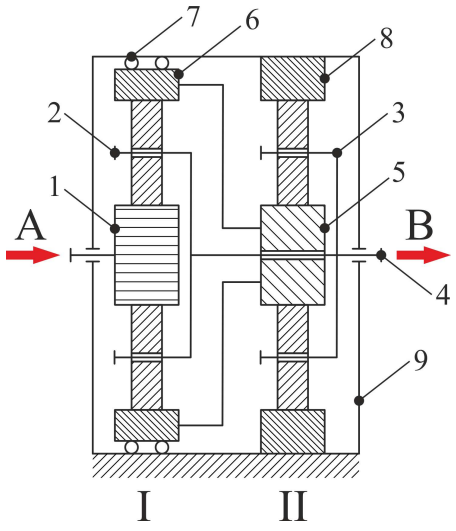

Figure 6. Kinematic scheme of S13WN planetary gear train.

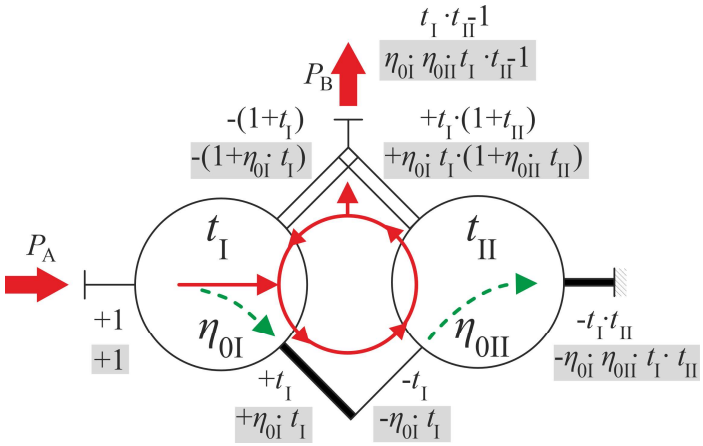

Figure 7. Power flow with ideal (white background) and real specific torques (gray background) for all PGT shafts of S13WN.

The analysis module detects possible solutions (combinations of ideal torque ratios) for layout variants which provide the requested transmission ratio. This data is used to create graphic representations of the interdependencies of different design parameters.

The first graph is presented in Figure 8, where it is possible to notice a considerable correlation of the x- and y-axis values. This is expected as it presents the correlation of maximum ring gear diameter and relation of maximum to minimum ring diameter: an increase at the y-axis implicates an increase at the x-axis, resulting in a cloud of points (x, y) in the x-y plane.

Other correlations from the analysis data are given in Figures 9, 10 and 11. In this case, every point in the domain (horizontal x-y plane) presents a pair of ideal torque ratios enabling an overall torque ratio in the desired range. The vertical (z) axis in Figure 9 presents the ratio of the sizes of the larger and smaller PGT ring gear diameters, which can variate between 1 and more than 4. Further analysis of the results confirms that PGTs with z - axis values equal or close to one will have minimal radial dimensions.

All points in the x-y plane of Fig 10 also present a pair of ideal torque ratios, while the maximal diameter of the transmission is presented on the z - axis.

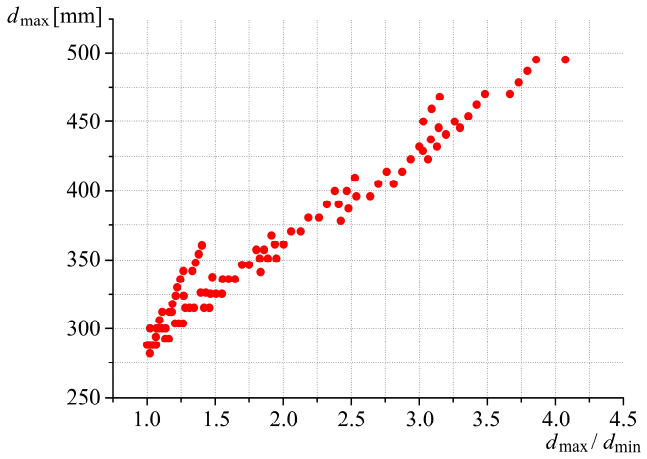

Figure 8. Correlation of maximum transmission diameter and relation of ring gear reference diameters for i = -30.

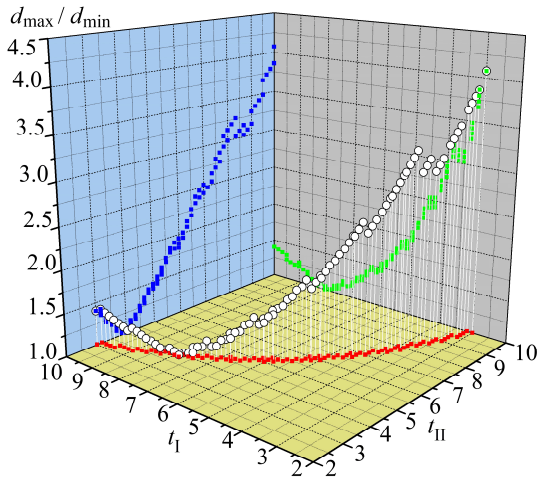

Figure 9. Influence of ideal torque ratios on the size ratio of the larger and smaller ring gear diameters for i = -30.

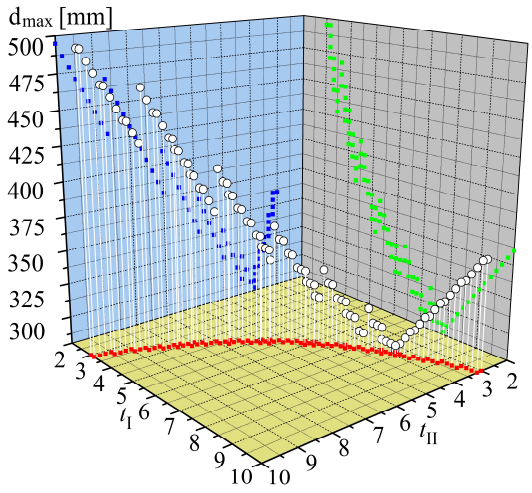

Figure 10. The influence of ideal torque ratios on maximal diameter of transmission for i = -30.

The z – axis in Figure 11 represents the overall efficiency of the PGT in relation to the combination of ideal torque ratios, and it can be concluded that efficiencies ranging from 0,944 to 0,969 can be achieved for torque ratios in the range from 2 to 10.

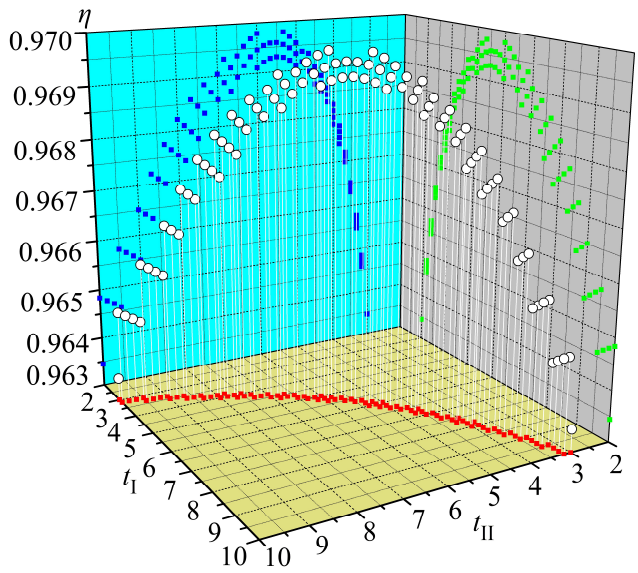

Figure 11. Influence of ideal torque ratios on overall efficiency for i = -30.

3.2 Application example 2

This case was calculated for the overall transmission ratio of i = -40. The analysis module has also found 16 suitable variants of transmissions which are reduced to 10 different variants due to isomorphy, identical to Example 1.

The research results were processed in the same way as in Example 1 and laid out in Table 2, taking into consideration the criteria of the housing shape, maximum transmission diameter and efficiency.

Table 2. Tabulated research results for i = -40.

Variant	t_I	t_{II}	d_{max}/d_{min}	d_{max}	η	m_I	m_{II}
S26WN	7.67	3.67	1.016	280.5	0.97	2	4.25
S16WE	7.83	4	1.021	288	0.97	2	4
S66NE	5.83	5.67	1.03	288.7	0.49	2.75	2.75
S55NE	3.83	4.33	1.06	292.5	0.97	4	3.75
S44NE	4.33	3.83	1.064	312	0.76	4	4.25
S23WE	8.83	4	1.039	318	0.97	2	4.25
S13WN	8.67	4.67	1.077	336	0.97	2	4
S33NE	6.83	6.67	1.025	338.2	0.50	2.75	2.75
S22NE	5.67	5.83	1.029	551.2	0.52	5.25	5.25
S33NE	6.67	6.83	1.025	615	0.47	5	5

The variant S13WN was chosen again for the same reasons as in Example 1.
In this case, there are 71 combinations of ideal torque ratio combinations fulfilling the design constraints for i =-40, and they enable different dependencies between design parameters to be shown in Figures 12, 13, 14, and 15.

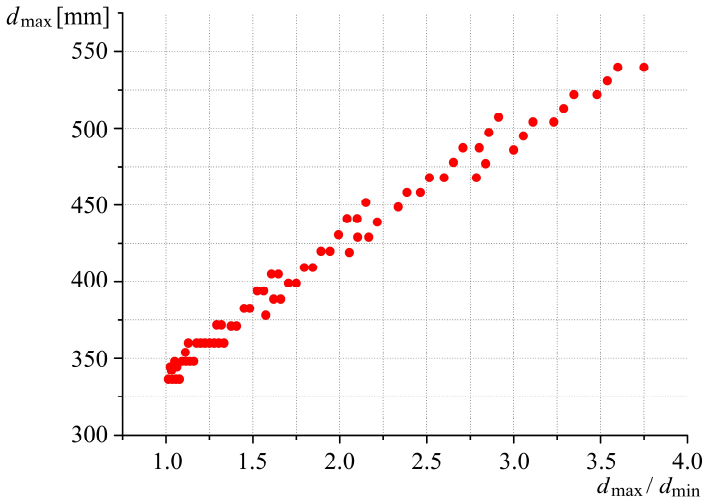

Figure 12. Correlation of maximum transmission diameter and relation of ring gear reference diameters for i = -40.

Figure 12 presents the relation of the maximum transmission diameter and maximum to minimum ring gear diameter ratio. It resembles Figure 8, as the y-axis increase is followed by an x-axis increase with the points (x, y) forming a cloud in the x-y plane. The difference is in the values at the x-axis and y-axis, as the maximum value on the y-axis is higher than the value in Figure 8, and the appropriate value at the x-axis is smaller than the value in Figure 8.

The size ratio of the larger and smaller PGT ring gear is presented at the z-axis of Figure 13, while the pairs of ideal torque ratios of the component gear trains are shown in the horizontal x-y plane. It is deducted from the chart shows that this ratio can variate between 1 and 4, and that the range of ideal torque ratios varies from 3 to 10.

Further analysis of the results also points that PGTs with z - axis values equal or close to unity will have minimal radial dimensions.

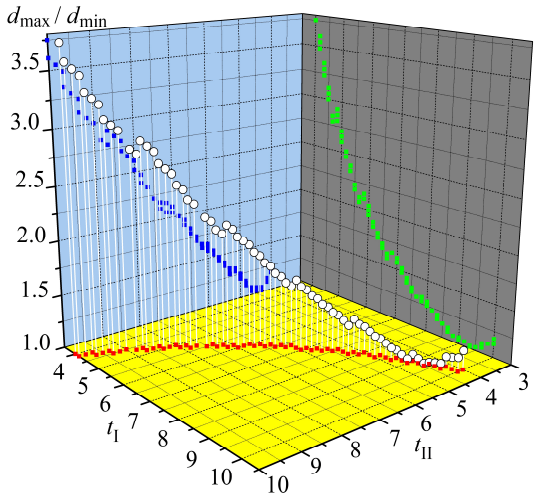

Figure 13. Influence of ideal torque ratios on the size ratio of the larger and smaller ring gear diameters for i = -40.

Every point in the x-y plane in Figure 14, presents a pair of ideal torque ratios (range from 3 to 10), while the z-axis presents the maximal diameter of transmission. The shape of the graph resembles Figure 9, with slightly larger values at the z-axis.

Figure 15 presents the relation of the ideal torque ratios are to the overall efficiency of the PGT. The z – axis in Figure 15 is used to represent efficiency, while the x-axis and y-axis are used to represent the horizontal plane. Efficiencies ranging up to 0,972 can be achieved for torque ratios in the 3 to 10 range, which is a slightly larger value in comparison with the value in Example 1.

The relation of the transmission efficiency to the overall transmission ratio, can be determined as in Figure 16. It has been determined that the efficiency increases with the transmission ratio for this PGT type. Furthermore, it can be concluded from the diagram in Figure 15 that PGTs with transmission ratios in the interval from -30 to -40 will have very small variations in efficiency, and that the variations at -40 are less pronounced than at -30, pointing to a small efficiency optimization window.

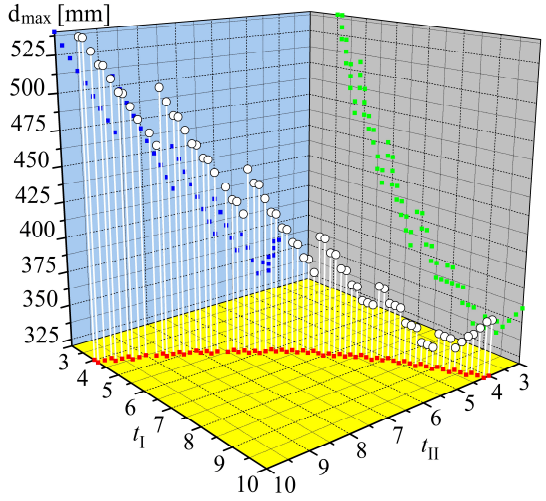

Figure 14. The influence of ideal torque ratios on maximal diameter of transmission for i = -40.

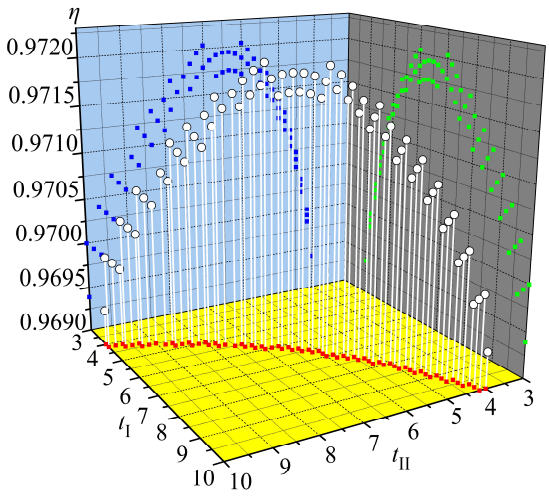

Figure 15. Influence of ideal torque ratios on overall efficiency for i = -40.

Furthermore, there is a slight increase in maximal diameter of the transmission at transmission ratio of -40 in comparison to the maximal diameter of transmission at transmission ratio of -30. The curves change in the same way for both calculation examples.

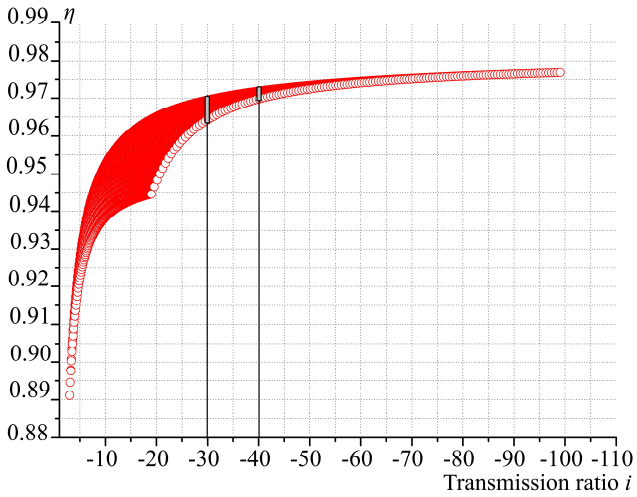

Figure 16. Influence of the overall transmission ratio on efficiency.

The results of the analysis performed in this paper show that two more variants are acceptable, however more detailed analysis is necessary. Those variants are S26WN and S16WE, shown in Figure 17 in addition to S13WN.

The input and output shafts of variant S16WE are on opposite sides, while variant S26WN is shown in an alternate configuration using the connecting outer ring gear shaft as the output.

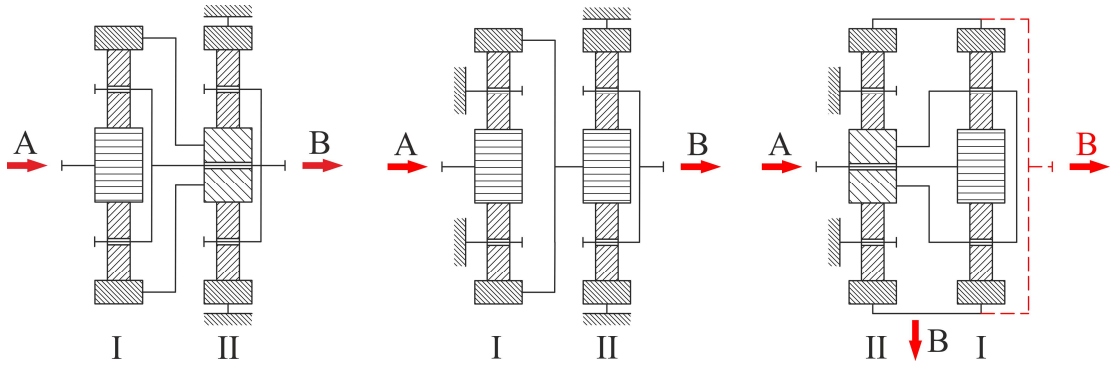

Figure 17. Schematic overview of S13WN (left) with alternate solutions S16WE (center) and S26WN (right, original output from Figure 5 indicated in dashed red).

Variant S16WE is in widespread use for marine propulsion and industrial applications, as both component PGTs of S16WE can be easily calculated independently of each other. On the other hand, the alternate configuration of S26WN, has found recent use as a high efficiency elevator worm gear drive replacement [35].

The comparison of the parameters of the variant S13WN with the other possible solutions S26WN and S16WE shows that the solutions S26WN and S16WE have better values for the maximum gear diameter, with satisfactory efficiencies. The ratios of the ring gear reference diameters are the same in all cases at a gear ratio of -30, while the solutions S26WN and S16WE have values closer to one at a gear ratio of -40, making them a better solution than S13WN. However, S13WN remains the better solution when the solution is selected according to technological requirements.

4 Conclusion

The analysis of a two-carrier PGT developed for a specific application, with transmission ratios of -30 and -40 is laid out in this paper. The application conditions require the use of the S13WN PGT. The variants and basic parameters of two-carrier drives within the application constraints were determined by means of the

DVOBRZ software package. The software package takes into consideration the design parameters such as gear geometry of the component gear trains, overall transmission ratio, average value of internal losses, gear material and overall efficiency.

The values of the different parameters for all valid calculated solution PGTs were stored as a function of the ideal torque ratios of the component gear trains. The resulting database was then used to select the best gearbox variant for the application first according to the criterion of minimal PGT dimensions, and second according to the criterion of maximum PGT efficiency.

The results of the analysis have shown that the efficiency of PGTs optimised for minimum size is negligibly smaller than in the case of optimization for maximum efficiency, however optimization for minimum size results in ease of manufacture as both ring gears will be of the same size.

Thorough analysis and comparison to all other kinematically equivalent PGTs has shown that S13WN does not present the best solution according to either criterion as both S16WE and S26WN have been determined to provide valid solutions according to both the criteria of minimum size and maximum efficiency. Another advantage of those variants in relation to S13WN is the absence of internal power circulation, resulting in a considerably lighter build. However, the application of variant S13WN is still recommended due to technological constraints and the fact that this variant has been thoroughly examined in literature.

References

[1] V. Jovanović, D. Janošević, and J. Pavlović, 'Analysis of the influence of the digging position on the loading of the axial bearing of slewing platform drive mechanisms in hydraulic excavators', *FU Mech Eng*, vol. 19, no. 4, p. 705, Dec. 2021, doi: 10.22190/FUME190225020J.

[2] A. Miltenović, M. Tica, M. Banić, and Đ. Miltenović, 'Prediction of temperature distribution in the worm gear meshing', *FU Mech Eng*, vol. 18, no. 2, p. 329, Jul. 2020, doi: 10.22190/FUME180120016M.

[3] J. Liu, R. Pang, H. Li, and J. Xu, 'Influence of support stiffness on vibrations of a planet gear system considering ring with flexible support', *J. Cent. South Univ.*, vol. 27, no. 8, pp. 2280–2290, Aug. 2020, doi: 10.1007/s11771-020-4449-0.

[4] Y. Park, W. Shi, and H. Park, 'Effect of the variable gear mesh model in dynamic simulation of a drive train in the wind turbine', *Eng. rev. (Online)*, vol. 41, no. 2, pp. 113–124, 2021, doi: 10.30765/er.1496.

[5] A. Goyal, V. Singh, and A. Patel, 'The analysis of material removal rate of WEDM miniature gears', *Eng. rev. (Online)*, vol. 41, no. 3, pp. 59–64, 2021, doi: 10.30765/er.1520.

[6] A. Dzyubyk et al., 'A new approach for evaluating the resistance of wheel steel to spall formation', *Eng. rev. (Online)*, vol. 40, no. 2, pp. 70–76, Apr. 2020, doi: 10.30765/er.40.2.08.

[7] A. Alexandrov, 'A Research and Comparative Analysis of the full Planet Engagement Planetary Gear Train', *TUS*, vol. 72, no. 1, Jun. 2022, doi: 10.47978/TUS.2022.72.01.006.

[8] S. Mohammed and L. A. Amina, 'Real-time friction torque estimation on a diesel engine using the crankshaft speed fluctuation', *Eng. rev. (Online)*, vol. 41, no. 3, pp. 42–58, 2021, doi: 10.30765/er.1515.

[9] D. Karaivanov, 'Theoretical and experimental studies of the influence of the structure of the coupled two-carrier planetary gear trains on its basic parameters', Ph. D. Thesis, University of Chemical Technology and Metallurgy, Sofia, 2000.

[10] V. N. Kudryavtsev and I. N. Kirdyiashev, *Planetary gear trains handbook*. Leningrad: Mashinostroenie, 1977.

[11] J. Looman, *Zahnradgetriebe: Grundlagen, Konstruktionen, Anwendungen in Fahrzeugen*, 3. neubearb. u. erw. Aufl. 1996, Nachdr. in veränderter Ausstattung. Berlin Heidelberg: Springer, 2009.

[12] H. W. Müller, *Die Umlaufgetriebe: Auslegung und vielseitige Anwendungen*, 2., Neubearb. und erw. Aufl. Berlin Heidelberg: Springer, 1998.

[13] K. B. Arnaudov and D. P. Karaivanov, *Planetary gear trains*. Boca Raton: Taylor & Francis, a CRC title, part of the Taylor & Francis imprint, a member of the Taylor & Francis Group, the academic division of T&F Informa, plc, 2019.

[14] 'Coupled two-carrier planetary gearboxes for two-speed drives', *Mach. Tech. Mat.*, vol. 15, no. 6, pp. 212–218, 2021.

[15] S. Troha, Ž. Vrcan, D. Karaivanov, and M. Isametova, 'The selection of optimal reversible two-speed planetary gear trains for machine tool gearboxes', *FU Mech Eng*, vol. 18, no. 1, p. 121, Mar. 2020, doi: 10.22190/FUME191129013T.
[16] J. Stefanović-Marinović, S. Troha, and M. Milovančević, 'An application of multicriteria optimization to the two-carrier two-speed planetary gear trains', *FU Mech Eng*, vol. 15, no. 1, p. 85, Apr. 2017, doi: 10.22190/FUME160307002S.
[17] M. Li, L. Xie, and L. Ding, 'Load sharing analysis and reliability prediction for planetary gear train of helicopter', *Mechanism and Machine Theory*, vol. 115, pp. 97–113, Sep. 2017, doi: 10.1016/j.mechmachtheory.2017.05.001.
[18] A. Kahraman, H. Ligata, K. Kienzle, and D. M. Zini, 'A Kinematics and Power Flow Analysis Methodology for Automatic Transmission Planetary Gear Trains', *Journal of Mechanical Design*, vol. 126, no. 6, pp. 1071–1081, Nov. 2004, doi: 10.1115/1.1814388.
[19] C. Chen, 'Power flow and efficiency analysis of epicyclic gear transmission with split power', *Mechanism and Machine Theory*, vol. 59, pp. 96–106, Jan. 2013, doi: 10.1016/j.mechmachtheory.2012.09.004.
[20] C. Liu, X. Yin, Y. Liao, Y. Yi, and D. Qin, 'Hybrid dynamic modeling and analysis of the electric vehicle planetary gear system', *Mechanism and Machine Theory*, vol. 150, p. 103860, Aug. 2020, doi: 10.1016/j.mechmachtheory.2020.103860.
[21] K. Arnaudov and D. Karaivanov, 'Engineering analysis of the coupled two-carrier planetary gearing through the lever analogy', in *Proceedings of the International Conference on Mechanical Transmissions*, Chongqing, China, 2001, pp. 44–49.
[22] S. Troha, 'Analysis of a planetary change gear train's variants', Ph. D. Thesis, University of Rijeka, Faculty of Engineering, Rijeka, 2011.
[23] D. P. Karaivanov and S. Troha, 'Optimal Selection of the Structural Scheme of Compound Two-Carrier Planetary Gear Trains and their Parameters', in *Recent advances in gearing: scientific theory and applications*, S. P. Radzevich, Ed. Cham: Springer, 2022, pp. 339–403.
[24] K. Arnaudow and D. Karaivanov, 'Systematik, Eigenschaften und Möglichkeiten von zusammengesetzten Mehrsteg-Planetengetrieben', *Antriebstechnik*, vol. 5, pp. 58–65, 2005.
[25] D. Karaivanov, A. Petrova, S. Ilchovska, and M. Konstantinov, 'Analysis of complex planetary change-gears through the torque method', *Mach. Tech. Mat.*, vol. 10, no. 6, pp. 38–42, 2016.
[26] Ž. Vrcan, J. Stefanović-Marinović, M. Tica, and S. Troha, 'Research into the Properties of Selected Single Speed Two-Carrier Planetary Gear Trains', *J. Appl. Comput. Mech.*, vol. 8, no. 2, pp. 699–709, 2022, doi: 10.22055/jacm.2021.39143.3358.
[27] Y. Ali, B. Mehmood, M. Huzaifa, U. Yasir, and A. U. Khan, 'Development of a new hybrid multi criteria decision-making method for a car selection scenario', *FU Mech Eng*, vol. 18, no. 3, p. 357, Oct. 2020, doi: 10.22190/FUME200305031A.
[28] D. Božanić, A. Ranđelović, M. Radovanović, and D. Tešić, 'A hybrid LBWA - IR-MAIRCA multi-criteria decision-making model for determination of constructive elements of weapons', *FU Mech Eng*, vol. 18, no. 3, p. 399, Oct. 2020, doi: 10.22190/FUME200528033B.
[29] J. Stefanović-Marinović et al., 'Optimization of two-speed planetary gearbox with brakes on single shafts', *Rep. Mech. Eng.*, vol. 3, no. 1, pp. 94–107, Dec. 2022, doi: 10.31181/rme2001280122m.
[30] D. Božanić et al., 'Modeling of neuro-fuzzy system as a support in decision-making processes', *Rep. Mech. Eng.*, vol. 2, no. 1, pp. 222–234, Dec. 2021, doi: 10.31181/rme2001021222b.
[31] M. Franulović, K. Marković, and A. Trajkovski, 'Calibration of material models for the human cervical spine ligament behaviour using a genetic algorithm', *FU Mech Eng*, vol. 19, no. 4, p. 751, Dec. 2021, doi: 10.22190/FUME201029023F.
[32] T. Todorov, R. Mitrev and I. Penev, 'Force analysis and kinematic optimization of a fluid valve driven by shape memory alloys', *Rep. Mech. Eng.*, vol. 1, no. 1, pp. 61–76, Sep. 2020, doi: 10.31181/rme200101061t.
[33] A. Pavlovic and C. Fragassa, 'Geometry optimization by fem simulation of the automatic changing gear', *Rep. Mech. Eng.*, vol. 1, no. 1, pp. 199–205, Dec. 2020, doi: 10.31181/rme200101199p.
[34] R. F. Handschuh, 'Epicyclic Gear Trains', in *Encyclopedia of tribology: with 3650 figures and 493 tablets*, Q. Wang and Y. Chung, Eds. New York: SpringerReference, 2013.
[35] L. Janovský, *Elevator mechanical design*, 3rd ed. Mobile, AL: Elevator World, 1999.